Defective Granule Exocytosis in Rab27a-deficient Lymphocytes from *Ashen* Mice

Elias K. Haddad,* Xufeng Wu,‡ John A. Hammer III,‡ and Pierre A. Henkart*

*Experimental Immunology Branch, National Cancer Institute; and ‡Laboratory of Cell Biology, National Heart, Lung, and Blood Institute, National Institutes of Health, Bethesda, Maryland 20892

Abstract. Because mutations in Rab27a have been linked to immune defects in humans, we have examined cytotoxic lymphocyte function in *ashen* mice, which contain a splicing mutation in Rab27a. *Ashen* cytotoxic T lymphocytes (CTLs) showed a >90% reduction in lytic activity on Fas-negative target cells compared with control C3H CTLs, and *ashen* natural killer cell activity was likewise diminished. Although their granule-mediated cytotoxicity pathway is profoundly defective, *ashen* CTLs displayed a normal FasL–Fas cytotoxicity pathway. The CD4/8 phenotype of *ashen* T cells and their proliferative responses were similar to controls. *Ashen* CTLs had normal levels of perforin and granzymes A and B and normal-appearing perforin-positive granules, which polarized upon interaction of the CTLs with anti–CD3-coated beads. However, rapid anti–CD3-induced granule secretion was drastically defective in both CD8$^+$ and CD4$^+$ T cells from *ashen* mice. This defect in exocytosis was not observed in the constitutive pathway, as T cell receptor–stimulated interferon-γ secretion was normal. Based on these results and our demonstration that Rab27a colocalizes with granzyme B-positive granules and is undetectable in *ashen* CTLs, we conclude that Rab27a is required for a late step in granule exocytosis, compatible with current models of Rab protein function in vesicle docking and fusion.

Key words: lymphocyte • cytotoxicity • Rab • exocytosis • myosin V

Introduction

Cytotoxic T lymphocytes (CTLs)[1] and natural killer (NK) cells lyse target cells by exocytosing specialized secretory granules containing perforin and granzymes into a synapse-like junction that forms between the lymphocyte and the bound target cell (Henkart et al., 1997; Stinchcombe and Griffiths, 1999). Death of the target cell requires perforin-dependent membrane permeabilization, followed by granzyme-dependent proteolysis of critical cytoplasmic substrates (Henkart et al., 1997). In addition to this granule-mediated pathway, CTLs also possess a second cytotoxic pathway in which T cell receptor (TcR) engagement induces expression of Fas ligand, which crosslinks Fas on the target cell surface, triggering apoptosis.

Several human diseases have been identified that involve defects in lymphocyte-mediated cytotoxicity via the granule exocytosis pathway. One such disease is Griscelli's syndrome, a rare autosomal recessive disease characterized by partial albinism in conjunction with other symptoms (Klein et al., 1994). Although the cause of this disease was originally identified as a mutation in the unconventional myosin, myosin Va (Pastural et al., 1997), recent work has shown that patients classified with this syndrome can have either of two different mutations (Menasche et al., 2000; Pastural et al., 2000). Although a small fraction of patients have mutations in myosin Va, the majority have mutations in Rab27a, a relatively uncharacterized Rab family member previously identified in melanocytes and cells of hematopoetic origin (Nagata et al., 1990; Chen et al., 1997). Rab GTPases reside on the surface of vesicles and organelles in the endocytic and secretory pathways, where they play critical roles in the targeting and fusion of these vesicles with their appropriate acceptor membrane by participating in the formation and/or function of SNARE complexes (Schimmoller et al., 1998; Chavrier and Goud, 1999). Importantly, although both types of Griscelli's patients exhibit partial albinism, only those with mutations in Rab27a exhibit T cell hyperproliferation and defects in lymphocyte cytotoxicity (Menasche et al., 2000).

Recently, the mouse coat color mutant *ashen* was shown to be caused by a mutation in Rab27a (Wilson et al., 2000).

Address correspondence to Pierre A. Henkart, National Institutes of Health, Bldg. 10, Rm. 4B36, Bethesda, MD 20892-1360. Tel.: (301) 435-6404. Fax: (301) 496-0887. E-mail: ph8j@nih.gov

[1]*Abbreviations used in this paper:* CTL, cytotoxic T lymphocyte; MLR, mixed lymphocyte reaction; NK, natural killer; poly I:C, polycytidylic-inosinic acid; TcR, T cell receptor; ZVAD-FMK, carbobenzoxy-valyl-alanyl-aspartyl (*O*-methyl)-fluoromethyl ketone.

Ashen mice exhibit a reduction in coat color intensity, an abnormal perinuclear distribution of melanosomes, the pigment-producing organelle of melanocytes, and a profound deficit in dense granules and their components within platelets. *Ashen* mice contain a single point mutation that prevents the proper splicing of Rab27a transcripts (Wilson et al., 2000). In an effort to define in a more precise way the role of Rab27a in lymphocyte-mediated cytoxicity, we have characterized CTLs from *ashen* mice with regard to granule biogenesis, distribution, and release, and with regard to cytotoxic function in vitro via the granule-mediated and Fas pathways.

Materials and Methods

Antibodies and Other Reagents

Unless otherwise specified, anti–mouse lymphocyte surface antibodies were purchased from BD PharMingen, as was recombinant IL-7. The sources of other antibodies were as follows: anti–mouse CTLA-4 (R&D Systems); antiperforin KM585 (Kamaya); anti–granzyme B (Santa Cruz Biotechnology, Inc.); anti-Rab27a (Signal Transduction Labs); and Texas red goat anti–rat IgG, donkey anti–goat IgG, and FITC-goat anti–mouse IgG (Jackson ImmunoResearch). Anti-CD3x–anti-TNP heteroconjugate was a gift from Dr. David Segal (National Cancer Institute, Bethesda, MD). The sources of other reagents were as follows: recombinant IL-2 (Boehringer); polystyrene beads (6.5 μm) (Polysciences, Inc.); carbenzoxy-valyl-alanyl-aspartyl (*O*-methyl)-fluoromethyl ketone (ZVAD-FMK) (Enzyme Systems); and concanamycin A (Alexis).

Mice, Cell Lines, and Lymphocytes

C3H/*ashen* mice and their parental strain C3H/HeSnJ (C3H), as well as C57Bl/6J (B6), were obtained from The Jackson Laboratory. B6 mice heterozygous for the *dilute* allele d[l20J], a functional null allele for the myosin Va heavy chain, were a gift of Neal Copeland and Nancy Jenkins (National Cancer Institute). The murine lymphomas L1210, L1210-Fas, and EL4 were maintained in RPMI 1640 supplemented with 10% FCS, 100 IU penicillin, and 10 μg/ml streptomycin. CTLs were generated from in vitro mixed lymphocyte cultures, which in the case of a*shen* and control C3H mice were established after priming with 2×10^7 EL-4 cells i.p. 10–14 d previously. Splenic responder cells from mutant and wild-type mice (1 ml at 2×10^6 cell/ml) were mixed with 1 ml of γ-irradiated stimulator spleen cells at 4×10^6 cells/ml (B6 for C3H and *ashen*, BALB/c for B6 and *dilute*). Cells were then cultured in 24-well plates in complete medium for 5 d at 37°C in 5% C0$_2$ incubator. Viable cells were isolated by lympholyte separation medium (Cedarlane Laboratories), and either used at this stage, or cultured for another 48 h in the presence of 0.8 ng/ml rIL-7 and 25 U/ml rIL-2 (7-d mixed lymphocyte reaction [MLR] cells). CD8$^+$ or CD4$^+$ cells were purified by positive magnetic bead selection using CD4 and CD8 microBeads and the VarioMac Cell sorting system (Miltenyi Biotec).

Cytotoxicity Assays, Granule Contents, and Degranulation

All target cells were labeled with Chromium-51 to detect lysis, and the CTL targets L1210 and L1210-Fas were TNP-modified by reaction with 1 mM trinitrobenzene sulfonate in PBS, pH 7.4, for 15 min to allow redirected lysis using 100 ng/ml anti-CD3x–anti-TNP heteroconjugate. Effector lymphocytes and 10^4 targets were incubated in 96-well plates for 4 h at 37°C in 5% C0$_2$, and the percent of supernatant Chromium-51 release was calculated with correction for background lysis. In some experiments, 50 μM ZVAD-FMK was added, whereas in others, CTLs were pretreated with concanamycin A (1 μM) for 2 h before being added to target cells in the continued presence of the drug. NK activity was measured on splenocytes harvested 24 h after i.p. injection of 50 μg of polycytidylic-inosinic acid (poly I:C) (Sigma-Aldrich). Proliferation of splenic T cells was measured by culture of splenocytes at 2×10^6/ml in complete medium in flat-bottom 96-well plates. For MLR, wells contained 4×10^6 irradiated C57Bl/6 splenocytes. For anti-CD3 induced proliferation, wells were pre-

coated with anti-CD3 (10 μg/ml) or a mixture of anti-CD3 plus anti-CD28. After 3 d, wells were pulsed with 5 μCi [^{3}H]thymidine for 8 h and harvested with a Mach IIM harvester (TOMTEC).

The granzyme A content of purified CD8$^+$ T cells was determined from 800 *g* supernatants of cells treated with 0.1% Triton X-100 for 10 min on ice. Its enzymatic activity was measured by addition of 100 μl of supernatant to 50 μl of 0.5 mM dithiobis-(2-nitrobenzoic acid) (Sigma-Aldrich) in 0.15 M NaCl, 0.01 M Hepes, pH 7.5, followed by addition of 50 μl of 200 μM of Cbz-lysine-thiobenzyl ester (Sigma-Aldrich). Absorbance at 405 nm was measured with a Victor Multiscan (Wallac Instruments) plate reader after 30 min at 21°C. The amounts of perforin, granzyme B, and Rab27a in purified CD8$^+$ cell lysates were estimated by Western blotting using ECL reagents (Amersham Pharmacia Biotech). To measure degranulation, purified CD8$^+$ or CD4$^+$ 7-d MLR T cells were added to flat-bottom wells coated with 10 μg/ml anti-CD3 or control hamster IgG, and supernatants were harvested at indicated times. For measuring degranulation by β-hexosaminidase release, supernatants (100 μl) were added to 100 μl of 1 mM methylumbelliferyl-*N*-acetyl-β-D-glucosaminide substrate (Sigma-Aldrich) diluted in 2% Triton-X 100 in 0.25 M citrate, pH 4.8. After incubation for 1 h at 37°C, the fluorescence (355/460 nm) was measured with the Victor plate reader. The supernatant β-hexosaminidase was expressed as a percentage of the total enzyme in 0.1% Triton X-100 lysates. The same supernatants were also tested for γ-IFN secretion by ELISA using mAb 37895.11 (Sigma-Aldrich) as a capture antibody and goat anti–mouse γ-IFN (Sigma-Aldrich) as a detecting antibody, with peroxidase-labeled pig anti–goat IgG (Sigma-Aldrich).

Flow Cytometry and Immunofluorescence

CD4/8 phenotyping was carried out by incubating 1 μg of appropriate antibody with 10^6 cells in 100 μl followed by flow cytometry with a FAC-Scan$^®$ (BD Biosciences). For anti–CTLA-4 staining, 7-d MLR cells were harvested and incubated with 10 μg/ml biotinylated anti–CLTA-4 antibody for 1 h. As a negative control, cells were incubated with 10 μg/ml nonbiotinylated anti-CTLA-4. Cells were then incubated with 1 μg of streptavidin-PE for 30 min and analyzed by flow cytometry.

For fluorescence microscopy, cells in suspension (10^6/ml) were plated in four-well poly-L-lysine chamber slides and fixed with 4% paraformaldehyde. Cells were then washed and blocked for 15 min in three changes of PBS containing 10% FCS. Cells were incubated sequentially for 1 h each in primary (1:100) and secondary antibodies (1:200) in blocking buffer containing 0.2% saponin (with a 15 min wash in between). After antibody staining, samples were washed and mounted using antifade mounting medium (SlowFade; Molecular Probes). Samples were viewed using a ZEISS LSM 510 confocal microscope.

Anti-CD3–coated beads were prepared by washing 6.5 μm polystyrene beads (Polysciences, Inc.) with PBS and then incubating overnight at 10^7/ml in PBS with 10 μg/ml purified anti-CD3 mAb 2C11. After washing, the beads were resuspended at 4×10^6 beads/ml in 0.5% BSA in HBSS. Purified CD8$^+$ 7-d MLR CTL at 8×10^6/ml were added at a 4:1 cell/bead ratio in this buffer. After incubation for the indicated time at 37°C, they were fixed, stained, and analyzed as above.

Results and Discussion

Defective Granule Exocytosis–based Cytolytic Activity in CTL and NK Cells from Ashen but Not Dilute Mice

CTLs from *ashen* mice were compared with C3H controls for their ability to lyse Fas-negative L1210 target cells using redirected cytotoxicity. *Ashen* CTLs showed a profound defect in target cell lysis, corresponding to >90% loss of lytic potency as seen by horizontal comparison of the titration curves (Fig. 1 A). A similar deficiency was observed using allospecific EL-4 target cells to measure direct TcR–mediated cytotoxicity (data not shown). NK activity of spleen cells from *ashen* mice was also decreased ~10 times compared with controls (Fig. 1 B). These results imply that Rab27a is expressed in both T cell and NK lymphocyte lineages and is required for cytotoxicity via the granule exocytosis cytotoxicity pathway.
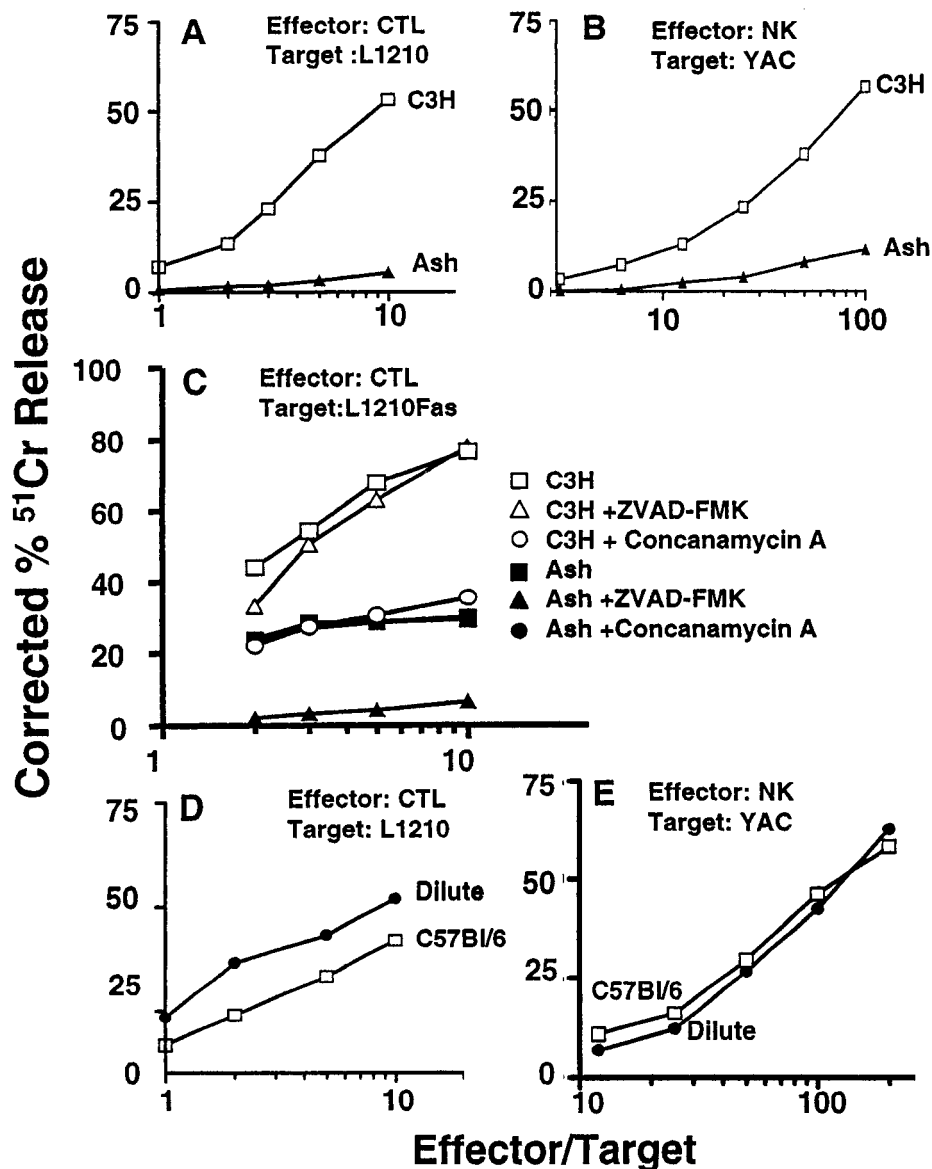
Figure 1. In vitro cytotoxicity of cytotoxic T and NK lymphocytes from *ashen* and *dilute* mice. (A) Activity of secondary CTL from *ashen* versus C3H control mice on Fas-negative L1210 targets, redirected with anti-CD3xanti-TNP. (B) NK activity of spleen cells from poly I:C–injected *ashen* versus C3H mice. (C) Activity of secondary CTLs from *ashen* versus C3H control mice on Fas-transfected L1210 targets, redirected with anti-CD3xanti-TNP. Solid circles are hidden by solid squares symbols in this graph. (D) Activity of primary CTLs from *dilute* versus C57Bl/6 control mice on Fas-negative L1210 targets, redirected with anti-CD3x–anti-TNP. (E) NK activity of spleen cells from poly I:C–injected *dilute* versus C57Bl/6 mice.

To examine if the FasL–Fas cytotoxicity pathway is defective in *ashen* CTLs, the cytotoxic activity of *ashen* CTLs on Fas-bearing target cells was examined. Fig. 1 C shows that *ashen* CTLs do kill a Fas-expressing transfectant of the L1210 target cells used in Fig. 1 A, although not nearly as well as do C3H controls. When concanamycin A was used to abolish the granule exocytosis cytotoxicity pathway (Kataoka et al., 1996), cytotoxic activity of C3H CTL was reduced to the level of *ashen* CTLs, which in turn was unaffected by this drug. These results show that the FasL–Fas cytotoxicity pathway is normal in *ashen* cells, whereas the granule exocytosis pathway is defective. In the presence of ZVAD-FMK, *ashen* CTLs showed no activity on L1210-Fas, confirming that this activity occurs via the FasL–Fas lytic pathway (Sarin et al., 1997). When both concanamycin A and ZVAD-FMK were added to the C3H CTL, lytic activity was totally abolished (data not shown). The lysis of L1210-Fas by *ashen* CTLs was not seen in the absence of anti-hapten–anti-CD3 heteroconjugate (data not shown), confirming

the requirement for TcR cross-linking for FasL expression in *ashen* CTLs. Together, these experiments show that *ashen* CTLs have an intact FasL–Fas cytotoxicity pathway even though their granule exocytosis cytotoxicity pathway is abolished, and argue against a general defect in TcR signaling in the *ashen* CTL. These results also suggest that the FasL detectable in perforin-containing CTL granules (Bossi and Griffiths, 1999) did not contribute significantly to the functional ligand on the effector cell surface in these experiments. This makes it unlikely that a defect in FasL surface expression due to compromised degranulation contributes to the T cell hyperproliferation in Griselli's patients with mutations in Rab27a, as might have been predicted from defects in FasL itself (Wu et al., 1996). Identical results to those shown in Fig. 1, A and C, were obtained with purified CD8^{+} CTL (data not shown).

Dilute and *ashen* mice exhibit identical degrees of coat color dilution and identical defects in the distribution of melanosomes within melanocytes (Wilson et al., 2000;

Parameter	C3H*	Ashen*
Thymocyte phenotype		
% CD4$^+$	5.9 ± 0.1	5.7 ± 0.2
% CD8$^+$	1.7 ± 0.5	1.7 ± 0.5
% CD4$^+$8$^+$	89.1 ± 3.1	88.9 ± 2.8
Splenocyte phenotype, ex vivo spleen		
% CD4$^+$	17.7 ± 2.1	16.5 ± 2.6
% CD8$^+$	10.2 ± 3.3	9.9 ± 4.2
Splenocyte phenotype, after 7 d MLR		
% CD4$^+$	14.8 ± 4.2	17.8 ± 9.8
% CD8$^+$	84.1 ± 11.6	81.7 ± 11.4
Spleen T cell proliferation‡		
MLR (αC57Bl/6)	6.6 ± 0.6	8.3 ± 1.1
α-CD3	13.3 ± 1.2	14.8 ± 1.0
α-CD3 + α-CD28	23.5 ± 1.8	23.1 ± 1.8

*Data shown are mean ± SD.
‡cpm × 10^3, day 3.

Wu et al., 2001). However, as shown in Fig.1, D and E, the cytotoxicity of CTL and NK cells from *dilute* mice is normal. Thus, exocytosis of cytotoxic lymphocyte granules does not appear to require myosin Va, in contrast to the generation of a proper peripheral accumulation of melanosomes within melanocytes, which requires both myosin Va and Rab27a. These data confirm in mice the results obtained in humans with mutations in either myosin Va or Rab27a, where only the latter exhibit defects in lymphocyte-mediated cytotoxicity (Menasche et al., 2000).

Ashen Thymocytes and Splenocytes Show Normal T Cell Phenotypes and Proliferative Responses

To determine whether the defective killing by *ashen* CTLs was due to a defect in T cell maturation, we compared T cell phenotypes of *ashen* and C3H spleens and thymus. Table I shows that *ashen* thymic and splenic T cells have a normal CD4/CD8 phenotype. Numbers of both thymocytes and splenocytes were identical in C3H and *ashen* mice (data not shown). MLR cultures showed similar expansion of CD8$^+$ cells with *ashen* and C3H splenocyte responders (Table I), and these CD8$^+$ cells showed similar increases in expression of the activation markers CD25 and CD44 (data not shown). *Ashen* and C3H splenic T cells also showed similar proliferative responses to alloantigen and anti-CD3 (Table I). Together, these data indicate that the defective killing by *ashen* CTLs is not due to obvious defects in T cell maturation or to a general defect in the expansion of precursors during effector cell differentiation.

Ashen CTLs Lack Rab27a but Contain Granules of Normal Morphology and Mediator Content

The defect in granule-mediated cytotoxicity exhibited by *ashen* CTLs implies that normal CTLs express Rab27a. The Western blot in Fig. 2 B shows that Rab27a is indeed present in C3H CD8$^+$ CTL but is undetectable in an equivalent load of *ashen* CTL extract. This lack of detectable Rab27a protein is compatible with the severe defect in processing of Rab27a transcripts seen by reverse transcriptase–PCR in tissues from *ashen* mice (Wilson et al., 2000).

The defect in the granule exocytosis cytotoxicity pathway in *ashen* cytotoxic lymphocytes could be due to a failure in the delivery of the critical effector proteins perforin and granzymes to the granules, or in the formation
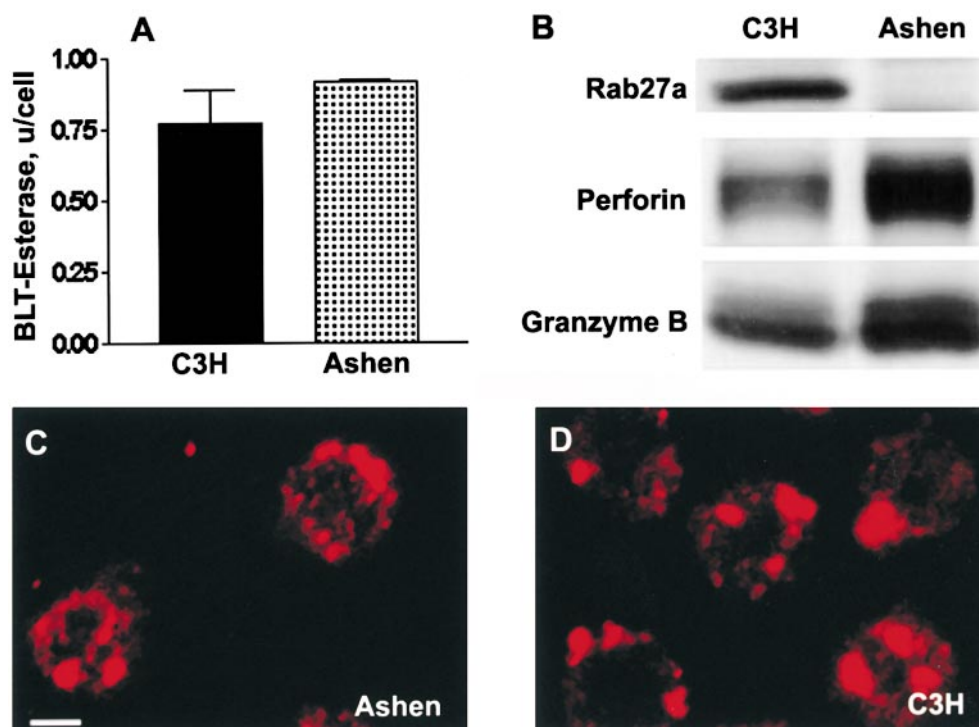

Figure 2. Expression of granule proteins and Rab27a in purified CD8$^+$ CTLs from *ashen* versus C3H control mice. (A) Granzyme A activity of Triton X-100 lysates of CTLs from *ashen* versus C3H control mice. Activity levels were determined from the linear portion of plots of activity versus cell number. (B) Western blot analysis of granzyme B, perforin, and Rab 27a from purified CD8$^+$ CTLs. (C and D) Immunofluorescent detection of intracellular perforin in *ashen* and C3H CTL, showing normal appearance of *ashen* CTL granules. Projected images are shown. Bar, 2.3 μm.
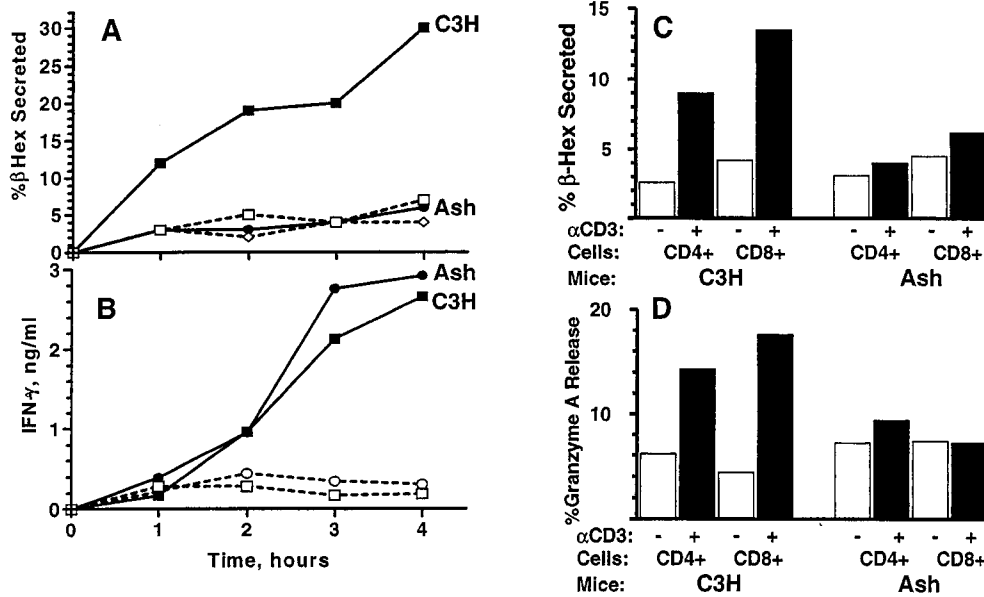
Figure 3. Anti-CD3 induced secretion in activated T cells from *ashen* versus C3H mice. T cells from 7-d secondary MLR cultures were incubated on wells coated with anti-CD3 or control hamster IgG. Secretion was determined from enzyme activity in supernatants, expressed as a percentage of levels in Triton X-100 cell lysates. (A) Time course of β-hexosaminidase release from *ashen* versus C3H T cells. (B) Supernatants from the experiment in A were analyzed for γ-interferon. (C) Purified CD4^{+} and CD8^{+} T cells were tested for β-hexosaminidase secretion after 4 h of incubation. (D) Secretion of the granule marker granzyme A in purified CD4^{+} and CD8^{+} after 4 h.

of the granules themselves, especially since platelets from *ashen* mice exhibit a dramatic reduction in the number of dense granules (Wilson et al., 2000). To address this possibility, we compared the levels of granule-expressed granzymes A and B and perforin in purified CD8^{+} CTL from *ashen* and C3H mice. Granzyme A enzymatic activity on a per cell basis was the same in *ashen* and C3H CTLs (Fig. 2 A). Granzyme B and perforin levels as determined by Western blot analysis (Fig. 2 B) were equal or greater in *ashen* CTLs relative to C3H controls. Furthermore, perforin-positive granules were present in similar numbers and appearance in *ashen* and C3H CTLs (Fig. 2, C and D). Therefore, we conclude that Rab27a is not required for the biogenesis of effector granules in CTLs.

The defect in the granule exocytosis cytotoxicity exhibited by *ashen* CTLs could also be due to the inability of granules to polarize to the site of target cell contact (Kupfer and Singer, 1989). We found that *ashen* CTLs can polarize their secretory granules upon contact with anti-CD3–coated beads (data not shown). Because this polarization is difficult to quantify, we cannot exclude the possibility that Rab27a contributes to the efficiency of this process, but we can conclude that it is not absolutely required for granule polarization to occur.

TcR-induced Granule Exocytosis Is Undetectable in CD8^{+} and CD4^{+} Ashen T Cells, Whereas Interferon-γ Secretion Is Normal

CTL granule exocytosis induced by TcR cross-linking can be measured by release of granule enzymes into the supernatant after incubation on anti-CD3–coated surfaces. Fig. 3 A shows that TcR-triggered granule exocytosis, measured by supernatant release of the granule marker β-hexosaminidase is undetectable in activated T cells from *ashen* mice. Fig. 3 B shows that when these same supernatants were analyzed for γ-interferon, which is rapidly secreted by the constitutive pathway after TcR cross-linking
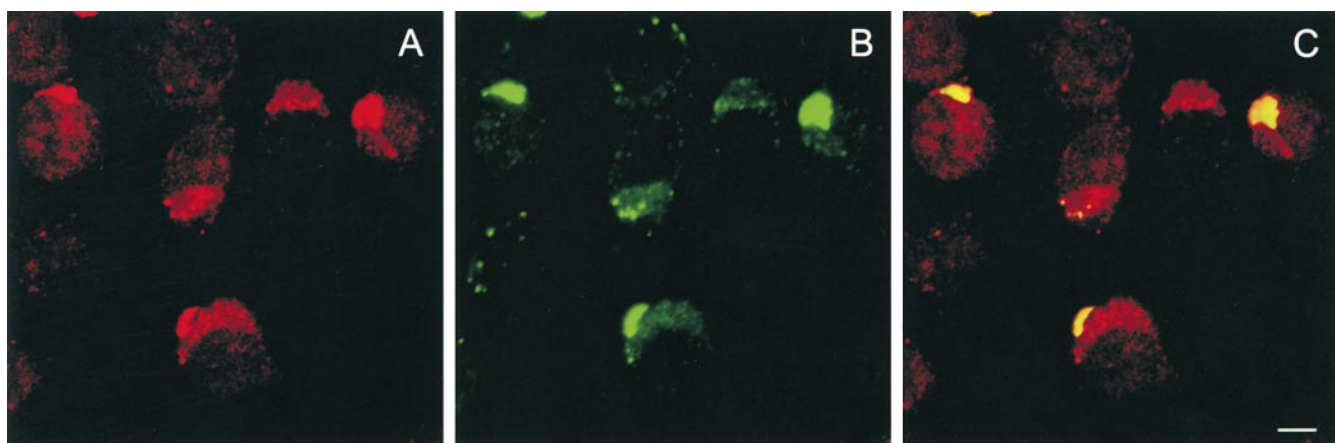

Figure 4. Immunofluorescence detection of Rab 27a and granzyme B in CD8^{+} C3H CTLs. (A) Granzyme B, red. (B) Rab 27a, green. (C) Colocalization of granzyme B and Rab 27a (yellow). Projected images are shown. Bar, 4.6 μm.
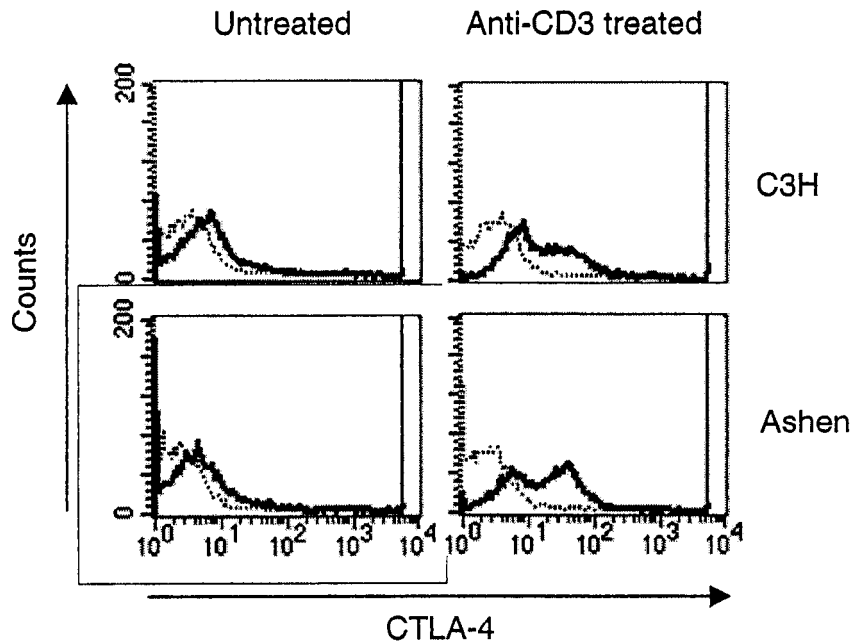
Figure 5. Anti-CD3 induced surface CTLA-4 expression in *ashen* versus C3H control mice. Secondary MLR-activated T cells from *ashen* and C3H mice were cultured on immobilized anti-CD3 for 4 h, stained for CTLA-4 without permeabilization, and analyzed by flow cytometry. Heavy line, cells stained with biotinylated anti–CTLA-4 and PE-streptavidin. Light line, cells stained with nonbiotinylated anti–CTLA-4 and PE-streptavidin.

(Fortier et al., 1989), no difference was observed between *ashen* and C3H CTLs. Thus, although Rab27a is required for the TcR-triggered exocytosis of granules containing preformed secretory products, it is not required for TcR-induced gene expression and exocytosis of the vesicles associated with the constitutive secretory pathway. These results also strengthen the case that TcR signaling is normal in *ashen* T cells.

Although lymphocyte granule exocytosis has been associated with cytotoxicity and has been described principally in $CD8^+$ T cells, we found that purified $CD4^+$ and $CD8^+$ T cells from 7-d MLR cultures have roughly equivalent levels of total β-hexosaminidase on a per cell basis. As shown in Fig. 3 C, when tested for TcR-stimulated secretion, purified activated $CD4^+$ as well as $CD8^+$ T cells from C3H mice showed a clear increase in supernatant release of β-hexosaminidase. However, comparable cells from *ashen* mice showed no secretion of this granule marker by either subpopulation. Fig. 3 D shows similar results for the granule marker granzyme A, which was also secreted in response to phorbol 12-myristate 13-acetate and ionomycin in C3H but not *ashen* CTLs (data not shown). Together with defective NK cytotoxicity (Fig. 1 B), our results show that $CD4^+$ and $CD8^+$ T cells, as well as NK cells, all require Rab27a for granule exocytosis. These data further extend the findings of defective granule exocytosis in activated T cells from Rab27a-deficient humans (Menasche et al., 2000).

Rab27a Localizes to Granzyme-containing Granules in CTLs

To determine whether Rab27a is present on cytotoxic lymphocyte secretory granules, we double stained $CD8^+$ CTLs for Rab27a and granzyme B. Fig. 4 shows that Rab27a exhibits strong colocalization with this effector granule marker, indicating that a large portion of cellular Rab27a resides on the surface of these granules.

TcR-induced Surface Expression of CTLA-4 Is Normal in Activated Ashen T Cells

After TcR ligation, T cells express CTLA-4 on their surface, which engages B7 family ligands and generates negative signals ending the interaction with antigen presenting cells. CTLA-4 knockout mice have a lethal lymphoproliferative disease (Waterhouse et al., 1995), confirming a role for CTLA-4 in limiting T cell proliferation. CTLA-4 has been localized to perforin-containing granules in $CD8^+$ CTLs (Linsley et al., 1996), and is expected to be expressed on the surface by a granule exocytosis process after TcR cross-linking. To assess the possibility that T cell hyperproliferation in Griscelli's patients bearing Rab27a mutations is due to a decrease in surface expression of CTLA4 secondary to defective granule exocytosis, we examined TcR-induced CTLA-4 surface expression in activated T cells from *ashen* and C3H mice. Fig. 5 shows that such cells from both strains have minimal basal CTLA-4 surface expression and that TcR cross-linking induces an equally large increase in surface CTLA-4 expression in both *ashen* and control T cells. Thus, a defect in CTLA-4 surface expression due to defective granule exoctyosis is unlikely to explain the hyperproliferation of T cells seen in Griscelli's syndrome patients with Rab27a mutations.

In conclusion, our results show that Rab27a functions at a late stage in the regulated secretion of granule mediators, but not in the constitutive secretory pathway. Unlike the case with platelet dense granule biogenesis, granules form normally in *ashen* CTLs and contain a normal complement of mediators. These granules polarize in response to TcR cross-linking and are associated with Rab 27a in wild-type CTLs. Our results argue that the principal site of action of Rab27a in the immune system is in cytotoxic lymphocytes and that it functions at a late step in the fusion of granules with the plasma membrane. This step could involve the Rab27a-dependent formation and/or function of the SNARE pair mediating granule–plasma membrane fu-

sion. Our results also shed light on the molecular etiology of the fatal human hyperproliferative syndrome resulting from mutations in Rab27a.

References

Bossi, G., and G.M. Griffiths. 1999. Degranulation plays an essential part in regulating cell surface expression of Fas ligand in T cells and natural killer cells. *Nat. Med.* 5:90–96.

Chavrier, P., and B. Goud. 1999. The role of ARF and Rab GTPases in membrane transport. *Curr. Opin. Cell Biol.* 11:466–475.

Chen, D., J. Guo, T. Miki, M. Tachibana, and W.A. Gahl. 1997. Molecular cloning and characterization of rab27a and rab27b, novel human rab proteins shared by melanocytes and platelets. *Biochem. Mol. Med.* 60:27–37.

Fortier, A.H., C.A. Nacy, and M.V. Sitkovsky. 1989. Similar molecular requirements for antigen receptor-triggered secretion of interferon and granule enzymes by cytolytic T lymphocytes. *Cell Immunol.* 124:64–76.

Henkart, P.A., M.S. Williams, C.M. Zacharchuk, and A. Sarin. 1997. Do CTL kill target cells by inducing apoptosis? *Semin. Immunol.* 9:135–144.

Kataoka, T., N. Shinohara, H. Takayama, K. Takaku, S. Kondo, S. Yonehara, and K. Nagai. 1996. Concanamycin A, a powerful tool for characterization and estimation of contributed of perforin- and Fas-based lytic pathways in cell-mediated cytotoxicity. *J. Immunol.* 156:3678–3686.

Klein, C., N. Philippe, F. Le Deist, S. Fraitag, C. Prost, A. Durandy, A. Fischer, and C. Griscelli. 1994. Partial albinism with immunodeficiency (Griscelli syndrome). *J. Pediatr.* 125:886–895.

Kupfer, A., and S.J. Singer. 1989. Cell biology of cytotoxic and helper T cell functions: immunofluorescence microscopic studies of single cells and cell couples. *Annu. Rev. Immunol.* 7:309–337.

Linsley, P.S., J. Bradshaw, J. Greene, R. Peach, K.L. Bennett, and R.S. Mittler. 1996. Intracellular trafficking of CTLA-4 and focal localization towards sites of TcR engagement. *Immunity.* 4:535–543.

Menasche, G., E. Pastural, J. Feldmann, S. Certain, F. Ersoy, S. Dupuis, N. Wulffraat, D. Bianchi, A. Fischer, F. Le Deist, and G. de Saint Basile. 2000. Mutations in RAB27A cause Griscelli syndrome associated with haemophagocytic syndrome. *Nat. Genet.* 25:173–176.

Nagata, K., T. Satoh, H. Itoh, T. Kozasa, Y. Okano, T. Doi, Y. Kaziro, and Y. Nozawa. 1990. The ram: a novel low molecular weight GTP-binding protein cDNA from a rat megakaryocyte library. *FEBS Lett.* 275:29–32.

Pastural, E., F.J. Barrat, R. Dufourcq-Lagelouse, S. Certain, O. Sanal, N. Jabado, R. Seger, C. Griscelli, A. Fischer, and G. de Saint Basile. 1997. Griscelli disease maps to chromosome 15q21 and is associated with mutations in the myosin-Va gene. *Nat. Genet.* 16:289–292.

Pastural, E., F. Ersoy, N. Yalman, N. Wulffraat, E. Grillo, F. Ozkinay, I. Tezcan, G. Gedikoglu, N. Philippe, A. Fischer, and G. de Saint Basile. 2000. Two genes are responsible for Griscelli syndrome at the same 15q21 locus. *Genomics.* 63:299–306.

Sarin, A., M.S. Williams, M.A. Alexander-Miller, J.A. Berzofsky, C.M. Zacharchuk, and P.A. Henkart. 1997. Target cell lysis by CTL granule exocytosis is independent of ICE/Ced-3 family proteases. *Immunity.* 6:209–215.

Schimmoller, F., I. Simon, and S.R. Pfeffer. 1998. Rab GTPases, directors of vesicle docking. *J. Biol. Chem.* 273:22161–22164.

Stinchcombe, J.C., and G.M. Griffiths. 1999. Regulated secretion from hemopoietic cells. *J. Cell Biol.* 147:1–6.

Waterhouse, P., J.M. Penninger, E. Timms, A. Wakeham, A. Shahinian, K.P. Lee, C.B. Thompson, H. Griesser, and T.W. Mak. 1995. Lymphoproliferative disorders with early lethality in mice deficient in Ctla-4. *Science.* 270:985–988.

Wilson, S.M., R. Yip, D.A. Swing, T.N. O'Sullivan, Y. Zhang, E.K. Novak, R.T. Swank, L.B. Russell, N.G. Copeland, and N.A. Jenkins. 2000. A mutation in Rab27a causes the vesicle transport defects observed in ashen mice. *Proc. Natl. Acad. Sci. USA.* 97:7933–7938.

Wu, J., J. Wilson, J. He, L. Xiang, P.H. Schur, and J.D. Mountz. 1996. Fas ligand mutation in a patient with systemic lupus erythematosus and lymphoproliferative disease. *J. Clin. Invest.* 98:1107–1113.

Wu, X., K. Rao, M.B. Bowers, N.G. Copeland, N.A. Jenkins, and J.A. Hammer. 2001. Rab27a enables myosin Va-dependent melanosome capture by recruiting the myosin to the organelle. *J. Cell Sci.* In press.